COBEM-2017-1116
HYBRIDIZATION OF CONCENTRATED SOLAR POWER AND CONFINED LANDFILL GAS FOR POWER GENERATION – A CASE STUDY

Arthur Monteiro Filho
Mario Benjamim Baptista de Siqueira
University of Brasilia, Department of Mechanical Engineering, Brasilia Brazil
arthurmtfilho@gmail.com, mariosiqueira@unb.br

Abstract. *Power generation is a subject much discussed today. There is still concerns about pollution from fossil fuels and a non-renewable characteristic of such fuels. With such growth it becomes necessary to study and understand new technologies and new sources of energy generation. Here, simulations were performed combining a linear-fresnel concentrated-solar- power system with gas extracted from a landfill to feed a 16 MWe thermoelectric power plant based on the estimated stock of gas by LandGEM model. The technology of choice was Integrated Solar Combined Cycle System (ISCCS). The calculation was carried out in a simplified way in order to obtain an estimate of the amount of gas needed to maintain the energy demand of the plant. The required flow rate was 34475t / year of methane required in the brayton cycle and 3209t/year by an auxiliary burner in bottoming Rankine Cycle. The solar component was 18% of heat needed for the Rankine system. The efficiency of the combined cycle obtained was about 42%.*

Keywords: *Hybridization, Urban Solid Waste, Landfill, Heliotherm Energy*

1. INTRODUCTION

Brazil and other under-developed countries have a history of inadequate garbage processing. Most of the urban solid waste is dumped in open areas with little to none planning (IBGE, 2010). After several years of piling up, landfill become an environmental hazardous (Carneiro, 2002). Besides toxic-liquid infiltration with possible water contamination, methane and other gases could escape to atmosphere in large quantities contributing to local air pollution and global warming (Figueiredo, 2016). On the other hand, the combustible gas could be harvested and used for electric energy generation offsetting fossil fuel consumption and green-house gas emissions.

Furthermore, the hybridization of energy-generating plants that use solar energy has been extensively studied over the last few years (Alqahtani and Dalia, 2016), (Hussain et al., 2017), (Coelho et al., 2015), (Tanaka et al.,2015), (Turchi and Zhiwen, 2014) and (Peterseim et al., 2014a). These studies seems to indicate the potential and feasibility of the hybridization of Concentrated Solar Power (CSP) technology with other energy sources (Peterseim et al., 2014b), including urban solid waste for energy generation (Spliethoff et al., 2010), and (Peterseim et al., 2012). There are investigations with the multiple solar technologies such as Linear Fresnel (Spliethoff et al., 2010), parabolic trough (Behar et al., 2014) and parabolic dish (McDonald, 1986).

For these reasons, it is proposed in this work, the study of a hybrid CSP-confined gas plant for power generation. In the study, a Linear Fresnel solar technology is combined with the confined-gas in the Jockey Club Brasilia landfill, one of the biggest in the Latin America, also known as "Lixão da Estrutural" to power a thermo-electric plant. Linear Fresnel was chosen because it represents less capital investment and can be easily expanded. For the simulation proposed here, it is necessary to estimate the amount of gas contained in the landfill. For this task, the United States Environmental Protection Agency (USEPA) methodology, called LandGEM, was used. This estimate guided the power-plant size and design.

2. COMPUTACIONAL PROCEDURE

For the study in question, it was determined that the plant should generate 16 MWe (electric) continuously. This size was chosen based on the amount of gas stocked and considering a 30-year operation of the plant. A Linear Fresnel solar plant was scaled with the aid of System Advisor Model (SAM), free software developed by the United States National Renewable Energy Laboratory (NREL). The plant considered was an Integrated Solar Combined Cycle System (ISCCS), shown in Fig. 1, which is maintained by burning the methane gas confined in the landfill in a Brayton Cycle. The gases from the burning pass through a superheater in order to overheat the steam in a Rankine Cycle. The stages of preheating and evaporation occur thanks to the heat supplied by the sun in a solar field using Linear Fresnel technology.

Each component in the cycle was modeled according to the required thermodynamic equations. Both gas- and vapor-turbines and the compressors were modeled according to the isentropic efficiency. The heat exchangers were sized using the ε-NUT method and the condenser of the Rankine cycle was sized by the Logarithmic Mean Temperature Difference. The thermodynamic model for the plant was implemented in Engineering Equation Solver (EES) and a one-year cycle was simulated using solar data from Solar Wind Energy Resource Assessment (SWERA) for Brasília.

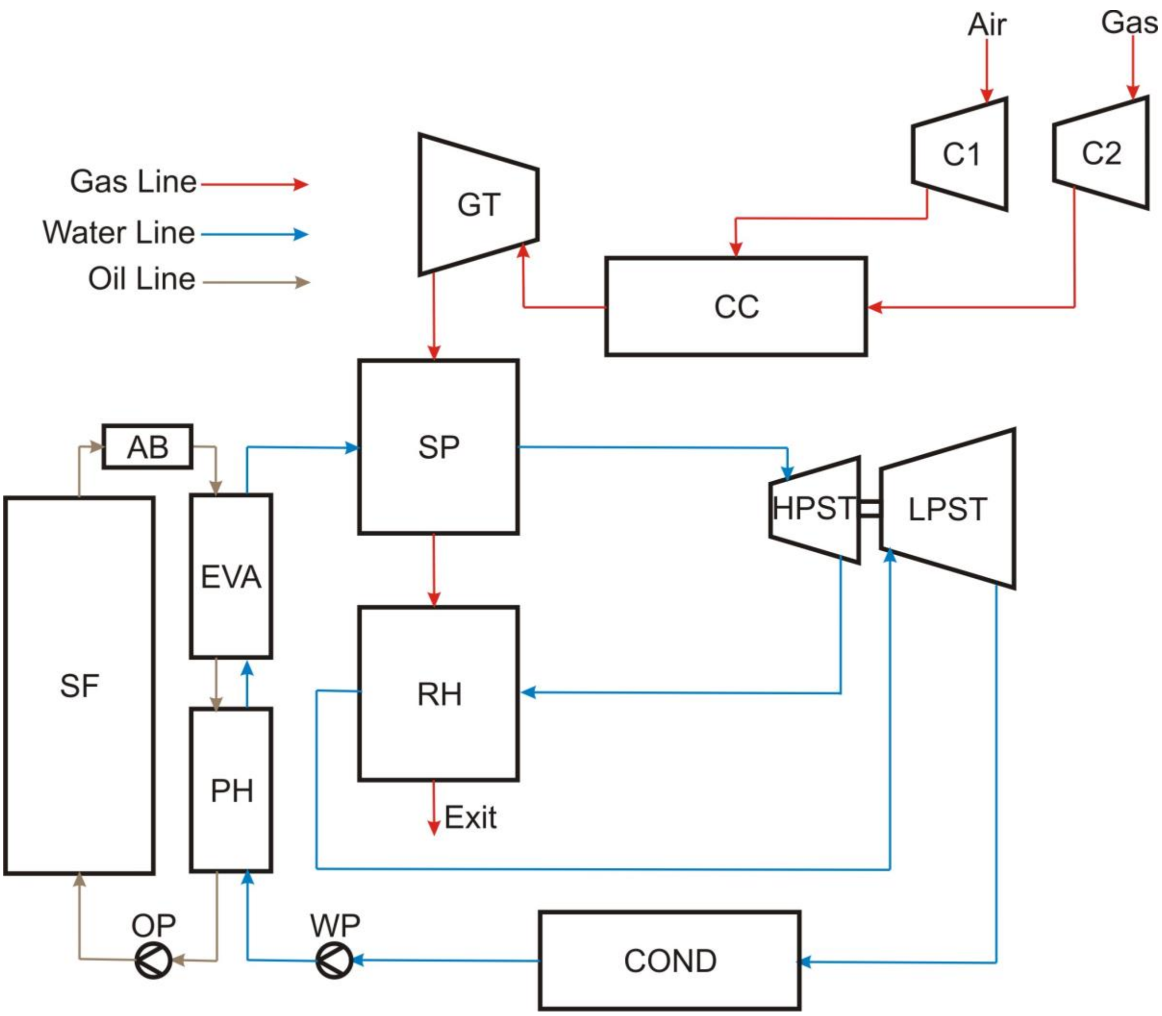

Figure 1: Scheme of the Integrated Solar Combined Cycle System simulated. C1-Air Compressor; C2-Gas Compressor; CC-Combustion Chamber; GT-Gas Turbine; SP-Superheater; RH-Reheater; HPST-Hogh-Pressure Steam Turbine; LPST-Low Pressure Steam Turbin; COND-Condenser; PH-Preheater; EVA-Evaporator; AB-Auxiliary Burner; SF-Linear Fresnel Solar Field

The thermodynamic Rankine cycle of the configuration proposed is represented in Fig. 2. The solar energy input of the proposed system is used to pre-heat (Q_{PH}) and evaporate (Q_{EVA}) the water. An auxiliary burner is introduced to compensate for lack of solar energy during low solar radiation periods.

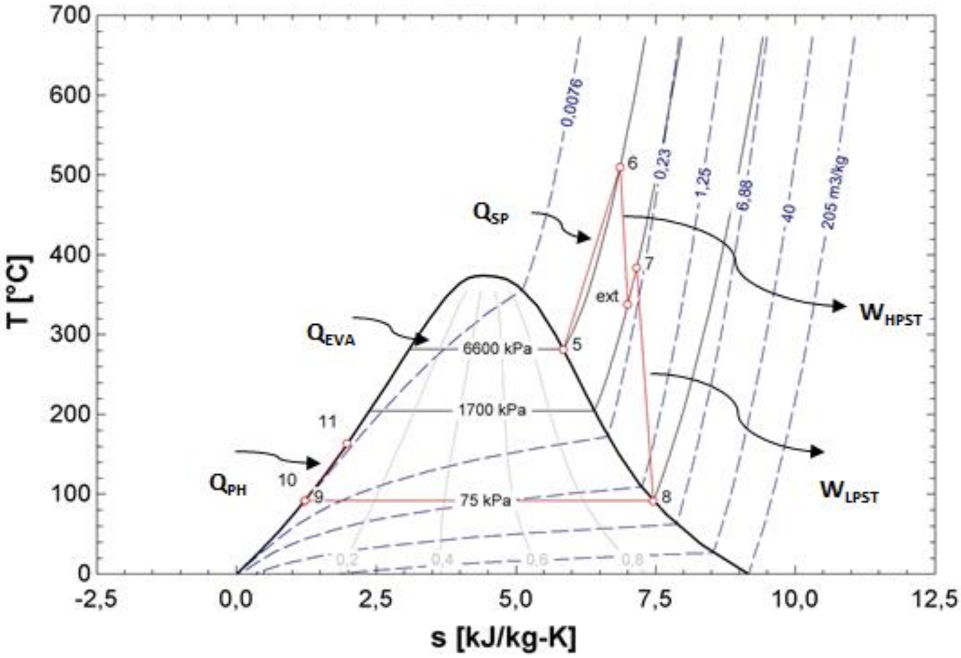

Figure 2: Diagram T-s for the Rankine cycle.

2.1 Solar Field

The Linear Fresnel solar field is a crucial component in the simulation. Its design should be as such that heat transfer fluid achieves temperatures high enough to power the Rankine cycle. Therefore, to simulate the Combined Cycle a solar field model is needed. The Solar Industrial Linear Fresnel LF-11 collector was used in the simulation. LF-11 schematic diagram with key dimensions on this collector is shown in Fig 3. Table 1 provides the complete data for the LF-11. This collector uses an individual tracking system for each mirror row to concentrate direct irradiation on an absorbed tube.

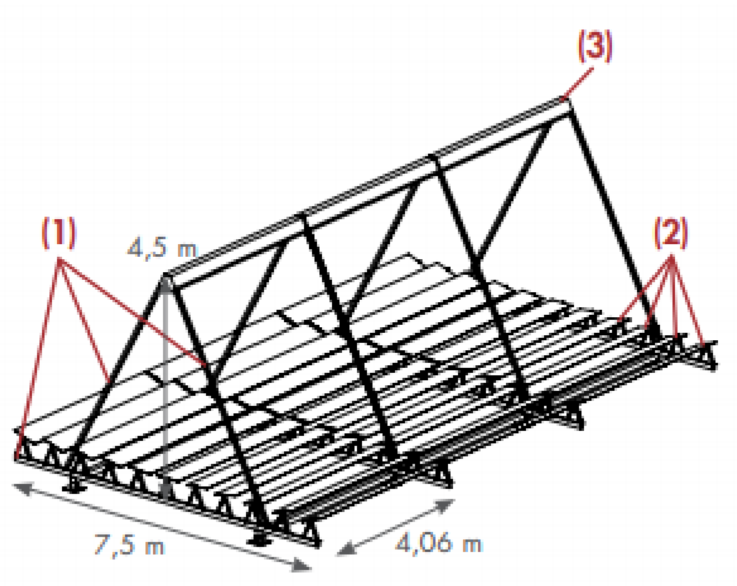

Figure 3: Schematic of the LF-11 solar collector.

The system physical and structural characteristics of the Linear Fresnel LF-11 provided by the supplier are presented in Tab. 1.

Table 1. Technical Data of the LF-11 Collector.

Data	**Value**	**Unit**
Module width	7,5	m
Module length	4,06	m
Aperture surface of primary reflectors	22	m²
Receiver height above primary reflector	4,0	m
Height of primary reflector above ground level	0,5	m
Recommended minimum clearance between parallel rows	0-0,5	m
Specific weight	27	Kg/m²
Maximum operational wind speed	100	Km/h
Maximum wind speed stowed	180	Km/h
Life expectancy	20	years
Maximum optical efficiency	0,663	-

The heat supplied by the solar collector is estimated by Eq. 2, which takes into account the solar direct normal irradiance (*DNI* [W/m^2]), the area of the collectors or the solar field (A_{SF} [m^2]) and optical efficiency:

$$Q_{solar} = \eta_{opt}.A_{SF}.DNI \tag{1}$$

The optical efficiency is an important feature of any solar collector and is a function of the modified incidence angles (*IAM*). For the present study the optical efficiency was calculated with Eq. 2, (Morin, 2012).

$$\eta_{opt} = \eta_{opt,\max}.IAM_L.IAM_T \tag{2}$$

The IAM's are in turn function of the solar elevation (α_s) and azimuth (γ_s) angles obtained from solar-earth geometric relationships (Sproud, 2007). Through the angles of elevation and azimuth the longitudinal (θ_l) and transverse (θ_t) incidence angles were calculated, Eq. 3 and Eq. 4, respectively.

$$\theta_l = \arccos(\sqrt{1-\cos^2(\alpha_s).\cos^2(\gamma_s)}\ ) \tag{3}$$

$$\theta_t = \arctan(|\sin(\gamma_s)| / \tan(\alpha_s)) \tag{4}$$

The collector manufacturer supplies the *IAM* data according to the angles of incidence, shown in Tab. 2.

Table 2: Incidence angles modifiers depending on the angles of incidence.

Angle	**Tranversal**	**Longitudinal**
0	1,000	1,000
05	1,044	0,962
10	1,000	0,937
15	1,034	0,907
20	0,996	0,867
25	1,015	0,821
30	0,998	0,768
40	0,956	0,640
50	0,951	0,485
60	0,784	0,311
70	0,553	0,141
80	0,300	0,022
90	0,075	0,000

Through polynomial regression with the data presented in Table 2, two equations were obtained for the *IAM* and are presented in Eq. 5 and 6.

$$IAM_T = 2{,}14450(10^{-9})\theta_t^5 - 4{,}3265(10^{-7})\theta_t^4 + 2{,}77324(10^{-5})\theta_t^3 - 7{,}48981(10^{-4})\,\theta_t^2 + 7{,}17058(10^{-3})\,\theta_t + 1{,}00503 \quad (5)$$

$$IAM_L = 4{,}78357(10^{-12})\theta_l - 1{,}15148(10^{-9})\theta_l + 1{,}46206(10^{-7})\theta_l - 9{,}68414(10^{-6})\theta_l + 1{,}68459(10^{-4})\theta_l - 7{,}09223(10^{-3})\theta_l + 0{,}998438 \quad (6)$$

By means of the obtained values of transversal angle of incidence in Eq. 4, it was possible to calculate by Eq. 5 the transverse incidence angle modifier. The same procedure occurred for the longitudinal incidence angle, calculated in Eq. 3. Since Eq. 6 was used to calculate the longitudinal incidence angle modifier.

The head losses on the absorber tubes were calculated by:

$$\Delta P = F \frac{L_{circuit}}{D} \rho_{fluid} \frac{\bar{V}^2}{2} \quad (7)$$

where ΔP is the pressure drop F is the Darcy´s friction factor, $L_{circuit}$ is the total length of the tubes, D is the tube diameter, ρ_{fluid} is the HTF density and $\bar{V}$ is the HTF mean velocity.

$$\bar{V} = \frac{4\dot{m}_{field}}{\pi D^2 \rho_{fluid} n_{circuits}} \quad (8)$$

where $n_{circuits}$ is the number of circuits in the Linear Fresnel solar field and $\dot{m}_{field}$ is the HTF mass flow within the solar field. Its value was estimated to sustain the heat transfer needed for the Rankine cycle. The value of F is calculated as function of tube roughness e given Eq. 9, (FOX et al., 2010).

$$\frac{1}{\sqrt{F}} = -1{,}8 \log_{10}\left[\left(\frac{\frac{e}{D}}{3{,}7}\right)^{1{,}11} + \frac{6{,}9}{\mathrm{Re}_{pipe}}\right] \quad (9)$$

with Reynolds number (Re)

$$\mathrm{Re}_{pipe} = \frac{\bar{V} D}{\mu} \quad (10)$$

Tab. 3 shows the values for these parameters used in the simulations.

Table 3. Values used and calculated for the solar field sizing.

Symbol	**Value**	**Unit**
D	0,07	m
$L_{circuit}$	975	m
e	0,00046	m
Re_{pipe}	187840	-
ρ_{fluid}	827,2	Kq/m^3
$\dot{m}_{field}$	36	Kg/s
$\bar{V}$	0,7539	m/s
F	0,3738	-
ΔP	1224	KPa
μ	2,809.10^{-7}	m²/s

2.2 LandGEM Method

The LandGEM method was developed by the USEPA for the estimation of emissions of gases from landfills. It is possible through this tool to evaluate the rates of generation of biogas, methane and carbon dioxide (Alexander et al., 2005).

The LandGEM method uses an Eq. 11 which is a first order decomposition rate equation. This equation is applied to estimate an amount of gas emitted for each year of inventory.

$$Q_{CH_4} = \sum_{i}^{n} \sum_{j=0,1}^{1} k L_o \left(\frac{M_i}{10} \right) e^{-k t_{ij}} \tag{11}$$

where Q_{CH4} [Mg/year] is the annual methane generation calculation, M_i [Mg] is the mass of waste accepted in the i_{th} year, L_o [m^3/Mg] is potential methane generation capacity, k [1/year] is methane generation rate, t_{ij} is age of the j_{th} section of waste mass M_i accepted in the i_{th} year and n is the number of years.

3. RESULTS AND DISCUSSION

The solar resource used by all CSP technology, given the fact that it requires the concentration of solar radiation, is *DNI*. Typical diurnal variation of *DNI* for each month in Brasilia is presented in Fig. 4. It reveals that the dry season (Jun-Sep), even though they are winter months, represents the best period for CSP generation due to the low cloudiness.

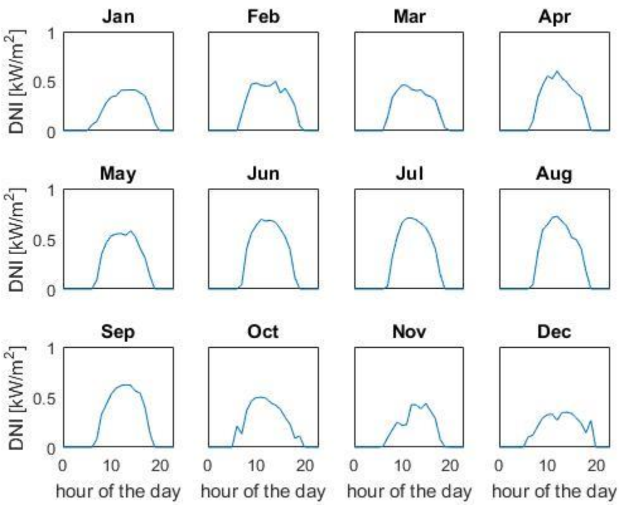

Figure 4: Diurnal variation of a typical day at each month in Brasilia.

For the design of the hybrid plant it was necessary to estimate how much methane would be available in the landfill. This estimation was carried out by applying the LandGEM Method proposed by the USEPA. Note that there was no availability of data and information necessary to consider gas losses over the years in the landfill. This lack of information is actually due to the non-controlled emissions in the landfill. Thus, it was assumed that there would be no loss of gas over the years, which means that the results presented here are overestimated. However, it offers an overview of possible energy generated through the available gas. The total methane used in the simulation is a sum of the generation of each year until 2017, which was the year considered as the year of closure of the landfill. After that, a decline would be expected due to the degassing.

Estimated methane quantity in the early years evolves rapidly. As for the maximum value, this method presented an amount of about 32 Gg/year of CH4 stored, value reached for the year 2017. To calculate the gas available for power generation in the Brayton cycle, the value obtained in this estimation was used. In order to do so, the values taken from the year of the landfill opening up to the year 2017 were summed; resulting in an estimated total amount of methane of 1034272 t. Fig. 5 shows the amount of methane generated in each year of this simulation.

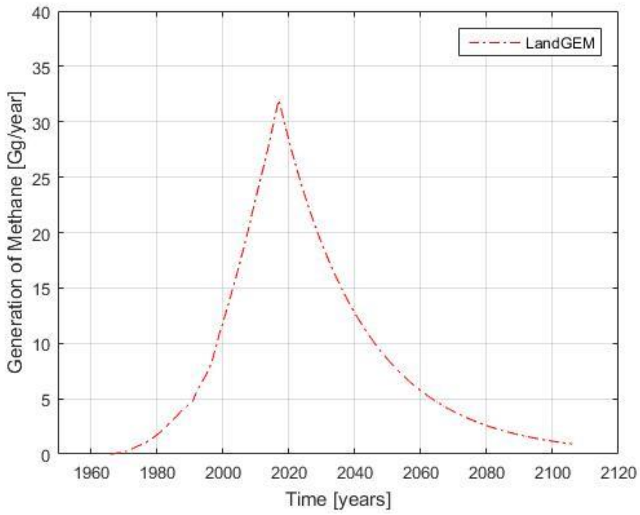

Figure 5: Methane generation estimate confined to the landfill over the years

To continuously supply of electric power intended for 30 years, the plant was designed to consume 34475 t/year of gas in the Brayton Cycle. With that in mind, the Rankine cycle would use the exhaust gas to superheat the vapour generated from the solar field. These constrain was used to configure the solar field and the Rankine cycle for maximum *DNI*. The auxiliary burner was used for the off design conditions.

The simulation was performed for an annual cycle of typical meteorological year. The power generation was maintained constant and use of gas in the auxiliary burner was estimated to off-set the lack of energy from the solar field during nighttime and unfavorable daytime conditions. Fig. 6 shows the contribution of the solar field and from the auxiliary burner for a clear-sky day during winter time and from a cloudy day during summer. It illustrates the different behavior of the plant as far as the contribution of solar energy to power generation.

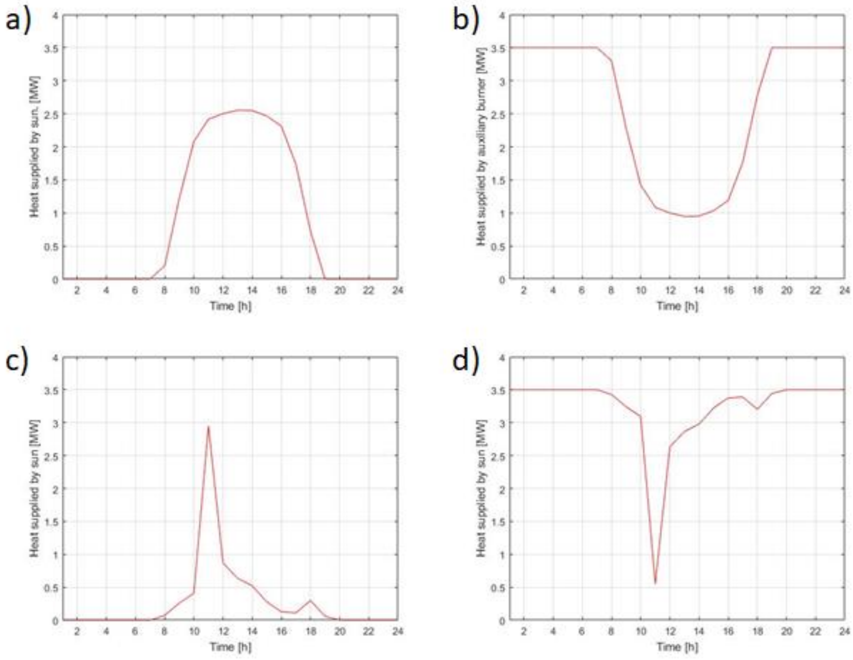

Figure 6: a) Heat supplied by Sun at August 17. b) Heat supplied by auxiliary burner at August 17 c) Heat supplied by Sun at January 25. d) Heat supplied by auxiliary burner at January 25.

Fig. 7 shows the monthly energy from the solar field and from the auxiliary gas burner. It is clear that the need of gas in the auxiliary system is considerable. This is because the plant is considered for base load, in other words, has to provide a firm power 24 hours each day. Because there is no storage, most of the gas is used during night time.

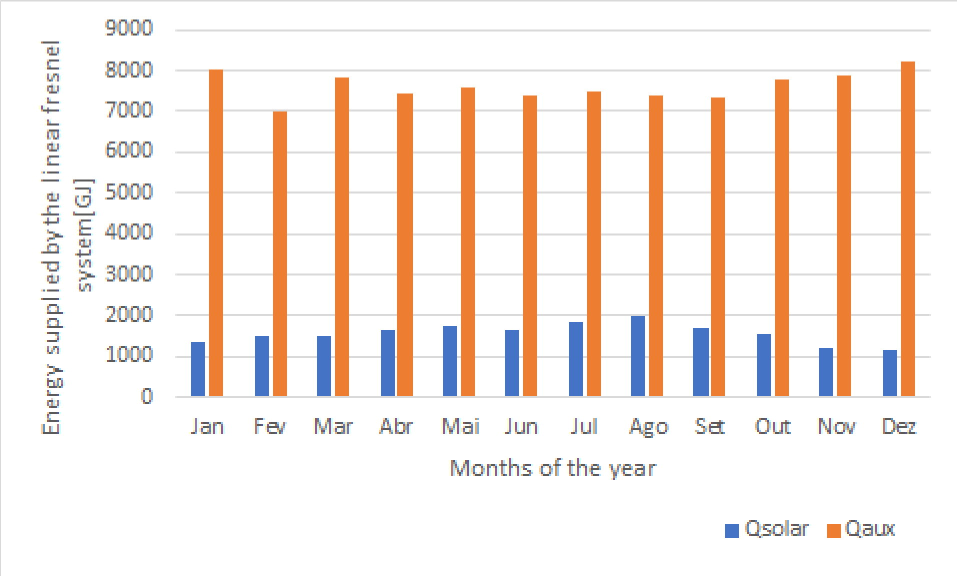

Figure 7: Total energy supplied by the linear Fresnel system and auxiliary burner monthly.

The hybridization was intended to augment the electric energy yield for the same amount of methane from the landfill. Tab. 1 shows the values of energy generated/consumed by the several components of the power system. From these values, the estimated efficiency of the combined cycle is 42%. The amount of gas consumed by the auxiliary burner 3209 t/y. Data shows that the Linear Fresnel was responsible for 18% of heat required for the Rankine cycle and 3% of the total heat of the combined cycle.

Table 4. Quantities of energy produced and consumed by the components of the generation plant.

Quantity	Symbol	Value	Unit
Energy supplied by Fresnel Linear System	Q_{Solar}	18991,86	GJ
Energy supplied by Auxiliary Burner	Q_{Aux}	91404,32	GJ
Energy consumed in the Methane Gas Compressor	W_{C2}	26461,86	GJ
Energy consumed in the Air Compressor	W_{C1}	107285,47	GJ
Energy generated in the Gas Turbine	W_{GT}	531791,47	GJ
Energy Consumed by the Rankine Cycle Pump	W_{RP}	1187,33	GJ
Energy Consumed by the Oil Pump	W_{OP}	2099,04	GJ
Energy generated in the high pressure stage of Steam Turbine	W_{HPST}	45285,70	GJ
Energy generated in the low pressure stage of Steam Turbine	W_{LPST}	62409,74	GJ
Energy released from methane burning in the combustion chamber	Q_{CC}	1083797,71	GJ

4. CONCLUSIONS

The simulations performed demonstrated that the combination of solar thermal technology and gas extracted from a landfill to generate electrical energy could be advantageous and strategic to mitigate environmental problems of decommissioning closed landfills. The solar field incremented the efficiency of the power cycle allowing more electric energy from the gas stored in the landfill, avoiding the environmental consequences of let the landfill abandoned after closing.

5. ACKNOWLEDGEMENTS

The authors appreciate CAPES for the financial support.

6. REFERENCES

Alexander, A., Burklin, C. E., & Singleton, A., 2005. Landfill gas emissions model (LandGEM) version 3.02 user's guide. US Environmental Protection Agency, Office of Research and Development.

Alqahtani, B. J., & Patiño-Echeverri, D., 2016. Integrated solar combined cycle power plants: paving the way for thermal solar. Applied Energy, 169, 927-936.

Behar, O., Khellaf, A., Mohammedi, K., & Ait-Kaci, S., 2014. A review of integrated solar combined cycle system (ISCCS) with a parabolic trough technology. Renewable and Sustainable Energy Reviews, 39, 223-250.

Carneiro, G. A., 2002. Estudo de contaminação do lençol freático sob a área do aterro de lixo do Jockey Club-DF e suas adjacências (Doctoral dissertation, Faculdade de Tecnologia da Universidade de Brasília.).

Coelho, B., Oliveira, A., Schwarzbözl, P., & Mendes, A., 2015. Biomass and central receiver system (CRS) hybridization: Integration of syngas/biogas on the atmospheric air volumetric CRS heat recovery steam generator duct burner. Renewable Energy, 75, 665-674.

Feldhoff, J. F., 2012. Linear Fresnel Collectors-A Technology Overview.

Figueiredo, M. C., Silva, S. M., & Neto, H. D. A. S., 2016. Avaliação de Impactos Gerados na Destinação Final de RSU Utilizando Análise do Ciclo de Vida: Estudo de Caso de Feira de Santana- BA.

Fox, R. W.; PritChard, P. J.; Mcdonald, A. T., 2010. Introduction to fluid mechanics. 7. ed. Hoboken, New Jersey: John Wiley & Sons.

Hussain, C. I., Norton, B., & Duffy, A., 2017. Technological assessment of different solar-biomass systems for hybrid power generation in Europe. Renewable and Sustainable Energy Reviews, 68, 1115-1129.

IBGE, 2010. Relatório, Pesquisa Nacional de Saneamento Básico 2008, Rio de Janeiro.

McDonald, C. F., 1986. A hybrid solar closed-cycle gas turbine combined heat and power plant concept to meet the continuous total energy needs of a small community. Journal of heat recovery systems, 6(5), 399-419.

Morin, G., Dersch, J., Platzer, W., Eck, M., & Häberle, A., 2012. Comparison of linear Fresnel and parabolic trough collector power plants. Solar Energy, 86(1), 1-12.

Peterseim, J. H., White, S., Hellwig, U., Tadros, A., & Klostermann, F., 2012. Concentrating Solar Power/Energy from waste hybrid plants-creating synergies. Proceedings of SolarPaces, SolarPaces.

Peterseim, J. H., Hellwig, U., Tadros, A., & White, S., 2014a. Hybridisation optimization of concentrating solar thermal and biomass power generation facilities. Solar Energy, 99, 203-214.

Peterseim, J. H., White, S., Tadros, A., & Hellwig, U., 2014b. Concentrating solar power hybrid plants–enabling cost effective synergies. Renewable Energy, 67, 178-185.

Reeken, F. V. et al., 2014. Report, Parabolic Trough CSP Technology State ot the Art and Market Overview.

Spliethoffs, H., Kaeding, N., Murer, M. Alonsoherranz, E., & Gohlke, O., 2010. Combining Energy from Waste and Concentrated Solar Power: New Solutions for Sustainable Energy Generation.

Sproul, A. B., 2007. Derivation of the solar geometric relationships using vector analysis. Renewable Energy, 32(7), 1187-1205.

Tanaka, Y., Mesfun, S., Umeki, K., Toffolo, A., Tamaura, Y., & Yoshikawa, K., 2015. Thermodynamic performance of a hybrid power generation system using biomass gasification and concentrated solar thermal processes. Applied Energy, 160, 664-672.

Turchi, C. S., & Ma, Z., 2014. Co-located gas turbine/solar thermal hybrid designs for power production. Renewable Energy, 64, 172-179.

7. RESPONSIBILITY NOTICE

The author(s) is (are) the only responsible for the printed material included in this paper.